

Statistical properties of underwater acoustic noise in Lake Hamrin, Diyala, Iraq

Thamer Easa Murad, Yasin Yousif Al-Aboosi

Department of Electrical Engineering, Collage of Engineering, Al Mustansiriyah Universit, Baghdad, Iraq

Article Info

Article history:

Received Jan 8, 2022

Revised Jul 9, 2022

Accepted Jul 29, 2022

Keywords:

Autocorrelation function
Gaussian distribution
Power spectral density
Underwater communication system
Wind noise

ABSTRACT

The greatest challenge in underwater acoustic communication systems is the minimization of underwater impact noise. This article offers an empirical example for determining the statistical properties of underwater acoustic noise in the in Lake Hamrin. The data are measured from various depths reached in Lake Hamrin, Diyala, Iraq. In most communication systems, noise is assumed to be additive as well as Gaussian. Underwater acoustic noise (UWAN) isn't only thermal noise, it also includes other components to the UWAN: turbulence, wind and shipping noises. Thus, it should be assumed that the acoustic noise is colored noise instead of white noise. Intermittent noise in the oceans and seas frequently includes significant Non-Gaussian elements. The samples noise data are analyzed in actual time for various depths of 1 meter, 3 meter and 5 meter in order to limit the statistical properties of underwater acoustic noise in Lake Hamrin, Diyala, Iraq such as the autocorrelation function (ACF), the probability density function (PDF) and also power spectral density (PSD). The experimental results showed that the noise of the Tigris river is a color noise and does not follow the Gaussian distribution.

This is an open access article under the [CC BY-SA](https://creativecommons.org/licenses/by-sa/4.0/) license.



Corresponding Author:

Thamer Easa Murad
Department Electrical Engineering, Mustansiriyah University
Falastin St, Baghdad, Iraq
Email: thamer1977@gmail.com

1. INTRODUCTION

Underwater communications are a key technology used in the ocean [1]-[3] for millions of years, in large oceans, some marine mammals such as dolphins and whales have used acoustic waves to communicate among themselves [4]. As of late, requests for underwater communications have increased because of the continued expansion of human actions in the underwater location. For example, observing the environment, toxic waste monitoring, exploring underwater, summation of scientific data, marine archaeology, offshore oil exploration, strategic observation [5]-[7], military issues, ocean exploration [8], and so on.

Common information medium for underwater communication includes radio waves, optical waves, magnetic waves and acoustic waves [9], [10]. Among them, the most popular medium for long distance communication is the acoustic wave because of its unique features in comparison to other applicants [11]. Radio waves are not preferable at low frequencies, as these waves are not able to travel long distances [12]. As a result of much higher attenuation in the water, and is rarely used for underwater communication [13]. Optical waves are not so attenuated, but are affected by absorption, scattering [14] and also high ambient light levels limiting the transmission range [15]. So, acoustic waves become the best option for short range and long range underwater communication [12].

Underwater noise is caused by three main factors: ambient or ocean background noise, vehicle noise and intermittent noise, including biological noise such as shrimps, ice cracking and rain [16]. Ambient noise may also be defined as a combination of various sources that are unable to uniquely identify [17]. Ambient noise seriously impairs acoustic communication [18]. Whereas ambient noise is frequently approached like Gaussian, in practice it is colored noise with a decaying power spectral density (PSD). This decay rate is about 18 (dB/decade). In contrast to ambient noise, intermittent noise frequently contains important Non-Gaussian elements [19]. Since the sound attenuation in the ocean depends upon the operating frequency, the ocean acts as a low pass filter (LPF) for background noise level. Therefore, PSD background noise is generally $(1/f)^n$ when the noise has lesser power at higher frequencies and greater power at lower frequencies [20]. There are a number of articles showing which noise isn't following a Gaussian distribution, especially in underwater communication systems. Underwater acoustic noise (UWAN) is characterized by the actual PDF with an extended tail shape, an emphasis on impulse behavior because of the high incidence of largeness amplitude noise events [16], [21].

2. UNDERWATER ACOUSTIC NOISE

There are four components to the UWAN: turbulence, shipping, wind and thermal noises. Each component has different frequency effects [22]. PSD is calculated as proportional to the operating frequency f (kHz) in (dB re micro Pa per Hz) [16], [21]. Turbulence noise $N_t(f)$ is generated in a system because the internal underwater movement, such as breakage waves [23]. The equation used to calculate turbulence noise is [24], [25].

$$N_t(f) = -30 \log f + 17 \quad (1)$$

Shipping noise is caused by heavy shipping in water [22]. It can be computed as [24], [26].

$$N_s(f, s) = 20(s - 0.5) + 26 \log f - 60 \log(f + 3 \cdot 10^{-2}) + 40 \quad (2)$$

Where: s represents the shipping activity factor between 0 (light) and 1 (heavy). The formula used to calculate wind noise is [27].

$$N_w(f, w) = 7.5\sqrt{w} + 20 \log f - 40 \log(f + 4 \cdot 10^{-1}) + 50 \quad (3)$$

Where:

w represents the wind speed in (m/sec) and is the wind factor with a value between 0 and 10. Thermal noise is a noise produced by randomly moving water molecules. It can be computed as [23].

$$N_{th}(f) = 20 \log f - 15 \quad (4)$$

The total power spectral density is the sum of thermal, wind, ship and turbulence and may be calculated using (5) [24], [28].

$$N_{\text{Total}}(f) = S_{xx}(f) = N_t(f) + N_s(f, s) + N_w(f, w) + N_{th}(f) \quad (5)$$

Figure 1 presents the experimental deep water, background (ambient) noise PSDs for various values of shipping activities ($s = 0, 0.5$ and 1) and wind speed with about (4.16 m/sec, 8 knots). Each noise source is found to be predominant within particular frequency range. $N_t(f)$ is dominant at very low frequencies generally (0.1-10 Hz), while $N_s(f, s)$ is the main factor contributing to noise in the frequency range (10-200 Hz). $N_w(f, w)$ is dominated in the frequency range (200-100,000 Hz). For frequencies above (100 kHz) thermal noise is dominant [22].

Figure 2 shows the experimental deep water noise PSD for various wind speeds ($w = 0, 5$ and 10) m/sec and shipping activities ($s = 0.5$). At fixed frequency, it is observed that the noise power spectrum density increases with increasing wind speed. Because, as the frequency increases, the effects of wind noise decrease. As a result, the dominance of that noise over a system becomes negligible [23]. However, this region is used by most acoustic systems [29]. When thermal noise is large the data rate is very bad. Basically the frequency choice criterion depends on the thermal noise value, since thermal noise is entirely dependent on the frequency of the signal. And since the frequency increases the thermal noise also increases [23].

These noise sources are dependent upon weather and other environmental factors. According to Figure 1 and Figure 2. The noise power spectrum lies in the region between both curves $(1/f)$ and $(1/f^3)$.

As a result, PSD background noise is generally $(1/f)^n$ when the noise has lesser power at higher frequencies and greater power at lower frequencies [20].

The UWAN in shallow water has more variation in time and location of deep waters. Consequently, modeling or predicting is more difficult. Shallow water environments include depths of up to 200 m, while deep water environments throughout the oceans and seas are considered to be at depths greater than 2000 m [30].

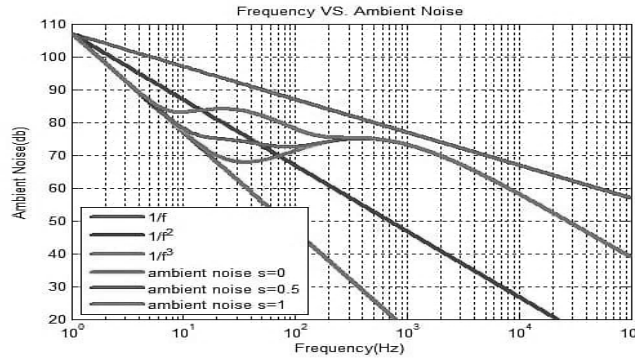


Figure 1. PSD noise in (dB re micro Pa per Hz) with $W = (4.16 \text{ m/sec, } 8 \text{ knots})$ and various shipping activities ($s = 0, 0.5 \text{ and } 1$)

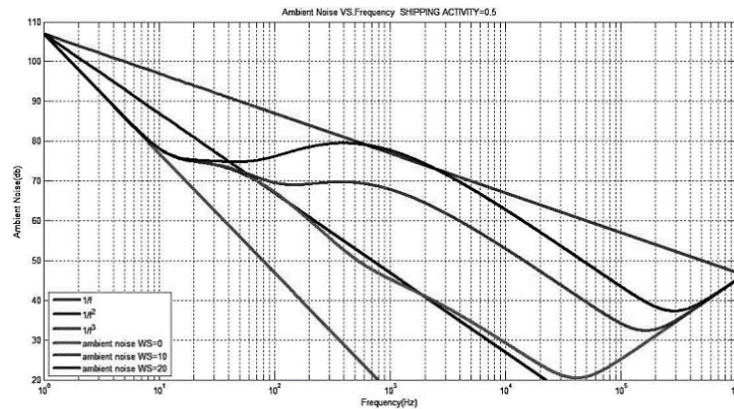


Figure 2. PSD noise in (dB re micro Pa/Hz) with different wind speeds ($w = 0, 5 \text{ and } 10$) m/sec and shipping activities ($s = 0.5$)

3. STATISTICAL PROPERTIES AND ESTIMATION

In contrast to deterministic signals, random signals have the best statistical properties. So, statistical properties are functions of autocorrelation, PSD and probability density function (PDF). Are explained in this document in details with equations.

3.1. Auto-correlation function

A random signal can be distinguished by the way in which it is valued at a given time T , is dependent upon a different time's value (τ, T). It is the autocorrelation function (ACF), which is the cross correlation between a signal and itself [30]. ACF can be found in (6).

$$R_{xx}(\tau, T) = E[x(T) x(\tau + T)] \tag{6}$$

Where: -

$E[\]$ represents an expected operator. When the random process is wide sense stationary (WSS), ACF may be represented as (7).

$$R_{xx}(\tau, T) = R(\tau) = E[x(T).x(\tau + T)] \tag{7}$$

The function is dependent on relative time instead of just absolute T. Within the normalized situation, $(0 \leq R_{xx}(\tau) \leq 1)$ which zero indicates that there is no dependence and another indicates high dependence [31].

3.2. Power spectral density and estimation

The power spectral density represents the frequency of random processes. PSD is estimated through estimating the power spectrum. Two types of power spectrum estimation (PSE) methods typically exist the first is parametric and the other is non-parametric. Contrary to parametric PSE, non-parametric PSE does not make any assumptions about the data generation process. The relationship of the ACF to the PSD is determined Based on the Wiener-Khinchine theorem [32].

$$S_{xx}(f) = \int_{-\infty}^{\infty} R_{xx}(t) e^{-j2\pi ft} dt, j=\sqrt{-1} \tag{8}$$

Equivalently,

$$R_{xx}(\tau) = \int_{-\infty}^{\infty} S_{xx}(f) e^{j2\pi f\tau} df \tag{9}$$

Letting $f = 0$ in (8) We get:

$$S_{xx}(0) = \int_{-\infty}^{\infty} R_{xx}(t) dt \tag{10}$$

In the same way, letting $\tau = 0$ in (9) Produces.

$$R_{xx}(0) = \int_{-\infty}^{\infty} S_{xx}(f) df \tag{11}$$

In (10) indicates that ACF is integrable if $(S_{xx}(0)$ is less than ∞) as well as (11) indicates that a PSD $S_{xx}(f)$ is integrable when $(R_{xx}(0)$ is less than ∞). Two equations are typical cases of conventionally color noise. Yet, this is various from color noise types $(\frac{1}{f^n})$ that have the property $(S_{xx}(0) \text{ equal } \infty)$ [31].

Five commonly used nonparametric spectrum estimation exists includes: the periodogram, the modified periodogram, Bartlett spectrum estimation, Welch spectrum estimation, and Blackman-Tukey spectrum estimation. The estimated power spectrum of the periodogram is limited because the periodogram is not a consistent power spectrum estimate in which the estimated white noise variance does not decrease with the signal length. Other ways are trying to minimize that problem. The Welch method is usually considered the most consistent PSE method. Welch method divides data from time series into segments (which may overlap) calculate a modified periodogram for each segment and calculate the average power spectrum density estimate. The average of the modified periograms tends to reduce the variance in the estimation of a single periodogram for all data recording. Segment overlap increases the number of segments, thereby reducing the variance. The signal is sampled by using a normalized sampling frequency, so Welch PSE is [32]:

$$P_{welch}(e^{jw}) = \frac{1}{KLU} \sum_{i=0}^{k-1} |w(n)X(n + iD)_e^{-jnw}|^2 \tag{12}$$

where:

K: NO. of segments, L: the length of each segment, D: the offset between two successive segments, L-D: NO. of overlapping points and U is the normalization factor. The standardization factor may be expressed as (13):

$$U = \frac{1}{L} \sum_{i=0}^{L-1} |w(n)|^2 \tag{13}$$

3.3. Probability density function

The standard noise model is Gaussian, additive, pixel independent and signal strength independent [33]. For many applications, Gaussian noise is mostly used as additive white noise for generating additive white Gaussian noise. This led to the probability distribution function given by:

$$P(z) = \frac{1}{\sigma\sqrt{2\pi}} e^{-\frac{(z-\mu)^2}{2\sigma^2}} \tag{14}$$

where μ : the mean value and σ : the standard deviation.

According to a number of publications, the UWAN does not follow the Gaussian (normal) distribution. Rather, UWAN is characterized by the with an extended tail shape reflecting an emphasis on impulse behavior because of the high incidence of largeness amplitude noise events [34]-[36]. UWAN is in accordance with the alpha-stable distribution class in which the characteristic equation is reversed. If we do not know the closed PDF format, the only solution is to use digital methods. Another modelling method involves empirically analyzing UWAN samples are taken from the seas and oceans [35]

Student t distribution associated with Gaussian distribution which is characterized with wide tails. Student t distribution is applied to calculate the population mean for a few samples and the standard deviation of the population is unknown. The student's t pdf is given by (15).

$$p_x(x) = \frac{\Gamma(\frac{\nu+1}{2})}{\sigma\sqrt{\nu\pi}(\frac{\nu}{2})} \left[\frac{\nu + \frac{(x-\mu)^2}{\sigma^2}}{\nu} \right]^{-\frac{\nu+1}{2}} \quad (15)$$

Where: $\Gamma(\cdot)$ represents the gamma function, μ represents the location parameter, σ represents the scaling parameter where ($\sigma > 0$), and ν represents the shape parameter where ($\nu > 0$), as ν increases, the t-distribution of the student is approaching a Gaussian distribution as shown in Figure 3.

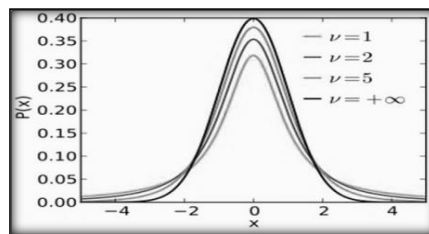


Figure 3. Probability gravity function of the t-distribution of student

4. RESULTS AND DISCUSSIONS

A number of noise samples were taken and collected from Lake Hamrin during experiences conducted at the, Diyala, Iraq. (Latitude: 34.07° N; longitude: 44. 5829° E) in 29 November 2021. The signals were received using a hydrophone with a range (20~20,000) Hz, model (Dolphin-EAR DE200 series), at various depths start with 1 meter, 3 meter and 5 meter to the bottom of the lake where the depth was 9 meter. Temperature (T) about 20 °C and W was about (4.16 m/sec, 8 knots). This is illustrated by Figures 4 to 6.



Figure 4. Trial location of the experiment



Figure 5. Field experiments in the Abu Dali district Tigris Beaches-Baghdad-Iraq, on 31 October 2020



Figure 6. Hydrophone model DolphinEAR DE200 series

UWAN is registered by the hydrophone model (Dolphin-EAR DE200 series), that they convert into a discrete time representation for more treating and store in a computer at type (PC). We can use a modified periodic diagram technique from Welch to estimate the energy spectrum as the data are analyzed for different depths of 1 m, 3 m 5 m and 7 m. Table 1 presents the details of the power spectrum estimation setup.

Factor	Value
Sample Frequency	8 KHz
Type of window	Hanning
Number of points	2048
Size of Window	256
Segment Length	64
Overlap percent	50%

Figure 7 Displays the waveform time representation and autocorrelation function of data collected from the two different depths of Figure 7(a) 3 m shows time representation of the underwater noise at depth 3meters, Figure 7(b) 5 m shows time representation of the underwater noise at depth 5meters, and Figure 7(c) 7 m shows time representation of the underwater noise at depth 7meters and its clearly its more impulsive behaviour than other depts. The number of noise samples is collected from Tigris River are considered correlated and colored noise due to the autocorrelation function of data collected is not like to the unit pulse This is different from white Gaussian noise. At $\tau = 0$, it represents the maximum magnitude of the noise power at ACF. Figure 8 describes the power spectrum estimation analyzed at various depths. It is obvious that UWAN has a decaying PSD. Whereas background (ambient) noise is frequently approached like Gaussian, in practice it is colored noise with a decaying PSD [19]. PSD background noise is generally $(1/f)^n$ when the noise has lesser power at higher frequencies and greater power at lower frequencies [20]. However, the power spectrum density isn't uniform over the entire range of frequencies of interest as shown in the Figure 8, So the noise is colored, but not white.

Figure 9. Demonstrates that the PSD of UWAN on a logarithmic scale with a deepness of 5 m is found from real field, where the rate of decay for the PSD of UWAN is about 20 (dB/decade). The actual field decay results compared to the [19] result differ by 2 (dB/decade), where the rate of decay for the PSD of ambient noise is about 18 (dB/decade). Figure 10. Indicates the PDF of UWAN found from the waveform time representation at a depth in Figure 10(a) 3 m shows pdf at depth 3m with degree of freedom 2.31, Figure 10(b) 5 m shows pdf at depth 5m with degree of freedom 2.82 and Figure 10(c) 7m shows pdf at depth 7m with degree of freedom 2.93 and at this depth its clearly the pdf of underwater noise fitting to non-Gaussian noise. Better t location-scale proper for PDF of sample noise with use the distribution fitting tool in the Matlab. The results of the comparison between the Gaussian distribution and the Student t distribution make it clear that the amplitude of the UWAN usually follows the t distribution of Student. In Table 2 indicates the degree of freedom for different depths 3, 5 and 7 meter. According to the Table 2, the average degree of freedom is approximately 2.687. It is observed that the values freedom Degrees are small which mean that UWAN does not follow the Gaussian (normal) distribution. Rather, UWAN is characterized by the with an extended tail shape reflecting an emphasis on impulse behavior because of the high incidence of largeness amplitude noise events [34]-[36]. The analysis demonstrated that the characteristics of the underwater acoustic noise do not similar the added white Gaussian noise. The probability density function of UWAN usually follows the t distribution of Student, unlike the supposition of a Gaussian probability density function suggested in a previous study [37].

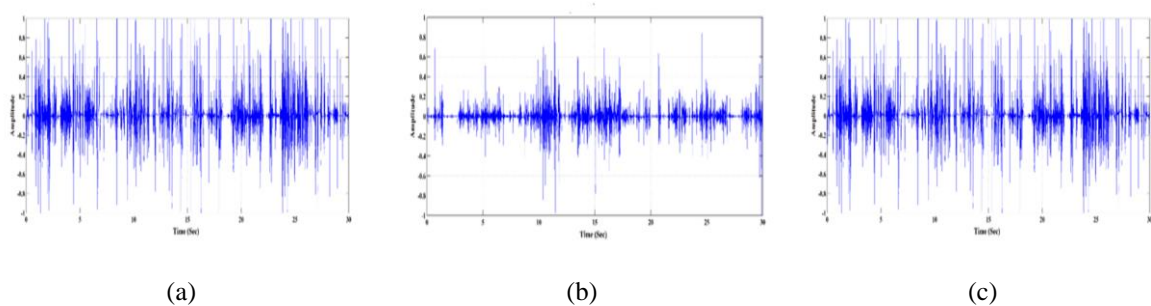


Figure 7. The waveform time representation and ACF of the UWAN for two various depths at (a) 3 m, (b) 5 m, and (c) 7m

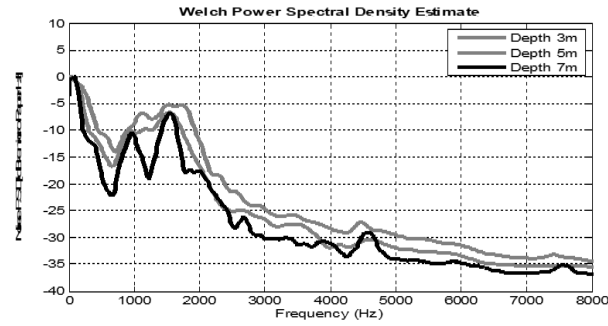


Figure 8. Welch PSD noise estimation at a depth 1 m, 3 m, and 5 m

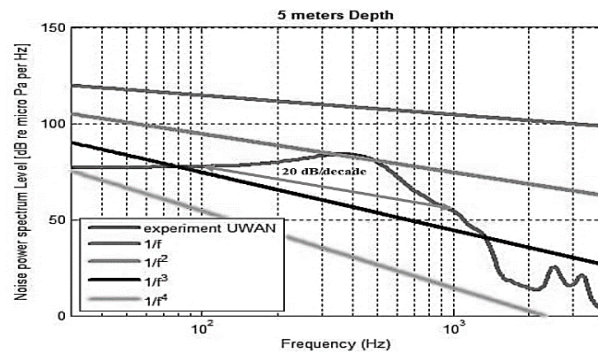


Figure 9. Welch PSD noise estimation at a depth of 5 m logarithmically

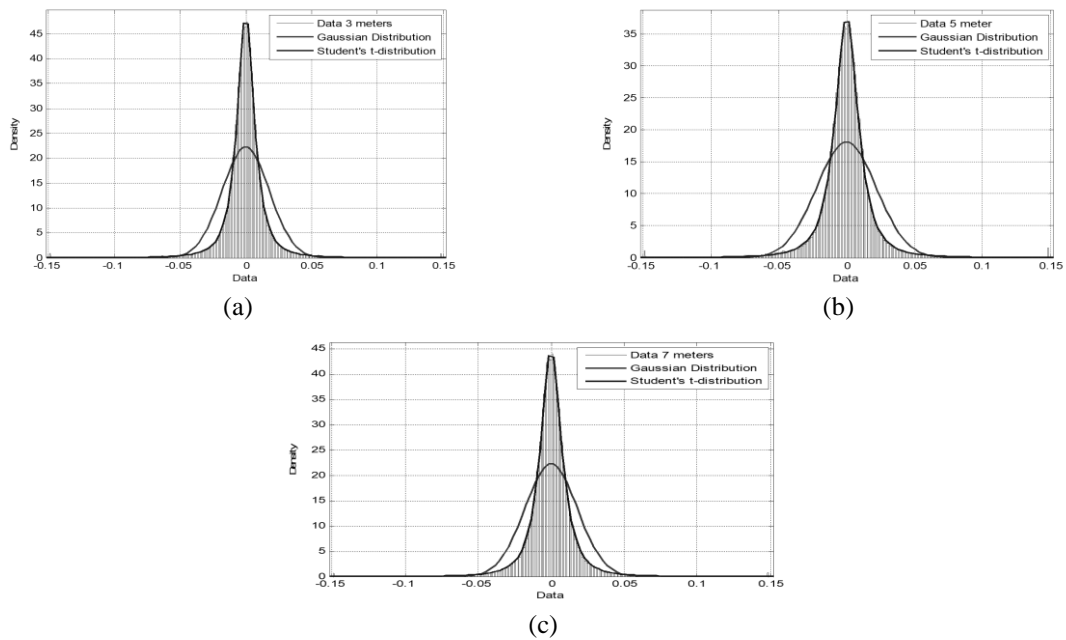


Figure 10. Comparison between the student's t -distribution and the Gaussian distribution for the probability density function of the real field samples noise at depths (a) 3 meter, (b) 5 meter, and (c) 7 meter

Different depths (m)	Freedom degrees (v)
3	2.31
5	2.82
7	2.93

5. CONCLUSION

The characteristics of the UWAN in Tigris River are particularly impulsive. PSD of the sample noise is taken from Lake Hamrin, Diyala, Iraq is not uniform over the entire frequency range and ACF of the sample noise isn't a delta function. Therefore, UWAN in Tigris River is considered colorful noise and Non-Gaussian distribution. Field trials presented that the noise power decreases from the surface of the lake to a depth of 5 meter, with a decay rate of about (20 dB/decade). The amplitude of the UWAN usually follows the t distribution of Student that is associated with the Gaussian distribution, but the tail's bigger. Consequently, UWAN does not take into account the assumption of white noise, meaning that Gaussian distribution is not applicable in the UWAN.

ACKNOWLEDGEMENTS

This work is supported by the college of Engineering/Mustansiriyah University (<https://webmail.uomustansiriyah.edu.iq>).

REFERENCES

- [1] H. Kaushal and G. Kaddoum, "Underwater optical wireless communication," *IEEE Access*, vol. 4, pp. 1518-1547, 2016, doi: 10.1109/ACCESS.2016.2552538.
- [2] Z. Zeng, S. Fu, H. Zhang, Y. Dong, and J. Cheng, "A survey of underwater optical wireless communications," *IEEE Communications Surveys & Tutorials*, vol. 19, no. 1, pp. 204-238, Firstquarter 2017, doi: 10.1109/COMST.2016.2618841.
- [3] J. Zhang, L. Kou, Y. Yang, F. He, and Z. Duan, "Monte-Carlo-based optical wireless underwater channel modeling with oceanic turbulence," *Optics Communications*, vol. 475, p. 126214, 2020, doi: 10.1016/j.optcom.2020.126214.
- [4] J. Li, "Advanced OFDM receivers for underwater acoustic communications," Ph.D. dissertation, University of York, 2017.
- [5] L. Lanbo, Z. Shengli, and C. Jun-Hong, "Prospects and problems of wireless communication for underwater sensor networks," *Wireless Communications and Mobile Computing*, vol. 8, no. 8, pp. 977-994, 2008, doi: 10.1002/wcm.654.
- [6] R. Headrick and L. Freitag, "Growth of underwater communication technology in the US Navy," *IEEE Communications Magazine*, vol. 47, no. 1, pp. 80-82, January 2009, doi: 10.1109/MCOM.2009.4752681.
- [7] K. Chen, M. Ma, E. Cheng, F. Yuan, and W. Su, "A survey on MAC protocols for underwater wireless sensor networks," *IEEE Communications Surveys & Tutorials*, vol. 16, no. 3, pp. 1433-1447, 2014, doi: 10.1109/SURV.2014.013014.00032.
- [8] X. Wang, X. Wang, R. Jiang, W. Wang, Q. Chen, and X. Wang, "Channel modelling and estimation for shallow underwater acoustic OFDM communication via simulation platform," *Applied Sciences*, vol. 9, no. 3, p. 447, 2019, doi: 10.3390/app9030447.
- [9] F. Hanson and S. Radic, "High bandwidth underwater optical communication," *Applied Optics*, vol. 47, no. 2, pp. 277-283, 2008, doi: 10.1364/AO.47.000277.
- [10] M. C. Domingo, "Magnetic induction for underwater wireless communication networks," *IEEE Transactions on Antennas and Propagation*, vol. 60, no. 6, pp. 2929-2939, 2012, doi: 10.1109/TAP.2012.2194670.
- [11] W. Sun, "Online learning of the spatial-temporal channel variation in underwater acoustic communication networks," Ph.D. dissertation, Michigan Technological University, 2019.
- [12] S. S. Panchal and J. P. Pabari, "Evaluation of shallow underwater acoustical communication model for attenuation and propagation loss for aqueous solution of sodium chloride," *2019 International Conference on Recent Advances in Energy-efficient Computing and Communication (ICRAECC)*, 2019, pp. 1-5, doi: 10.1109/ICRAECC43874.2019.8995039.
- [13] S. JIANG, *Wireless networking principles: from terrestrial to underwater acoustic*, Singapore: Springer, 2019.
- [14] L. Liao, "Underwater acoustic localization with applications to multiuser communications," Ph.D. dissertation, University of York, 2018.
- [15] S. Al-Dharrab, M. Uysal, and T. M. Duman, "Cooperative underwater acoustic communications [accepted from open call]," *IEEE Communications Magazine*, vol. 51, no. 7, pp. 146-153, 2013, doi: 10.1109/MCOM.2013.6553691.
- [16] G. Burrowes and J. Y. Khan, "Short-range underwater acoustic communication networks," in *Autonomous Underwater Vehicles*, London: IntechOpen, 2011.
- [17] D. H. Cato, "Ocean ambient noise: its measurement and its significance to marine animals," *Proceedings of the Institute of Acoustics*, vol. 30, no. 5, pp. 1-9, 2008.
- [18] N.-S. N. Ismail, L. A. Hussein, and S. H. S. Ariffin, "Analyzing the performance of acoustic channel in underwater wireless sensor network (UWSN)," *2010 Fourth Asia International Conference on Mathematical/Analytical Modelling and Computer Simulation*, 2010, pp. 550-555, doi: 10.1109/AMS.2010.111.
- [19] M. Stojanovic and J. Preisig, "Underwater acoustic communication channels: Propagation models and statistical characterization," *IEEE Communications Magazine*, vol. 47, no. 1, pp. 84-89, 2009, doi: 10.1109/MCOM.2009.4752682.
- [20] M. Chitre, J. Potter, and O. S. Heng, "Underwater acoustic channel characterisation for medium-range shallow water communications," *Oceans '04 MTS/IEEE Techno-Ocean '04 (IEEE Cat. No.04CH37600)*, 2004, pp. 40-45 Vol.1, doi: 10.1109/OCEANS.2004.1402892.
- [21] T. Melodia et al., "Advances in underwater acoustic networking," in *Mobile Ad Hoc Networking: Cutting Edge Directions*, Wiley Online Library, 2013.
- [22] Y. Y. Al-Aboosi, R. S. Issa, and A. K. Jassim, "Image denosing in underwater acoustic noise using discrete wavelet transform with different noise level estimation," *TELKOMNIKA Telecommunication, Computing, Electronics and Control*, vol. 18, no. 3, pp. 1439-1446, 2020, doi: 10.12928/telkomnika.v18i3.14381.
- [23] F. Pignieri, F. De Rango, F. Veltri, and S. Marano, "Markovian approach to model underwater acoustic channel: Techniques comparison," *MILCOM 2008-2008 IEEE Military Communications Conference*, 2008, pp. 1-7, doi: 10.1109/MILCOM.2008.4753161.
- [24] Y. Y. Al-Aboosi, A. Kanaa, A. Z. Sha'ameri, and H. A. Abdualnabi, "Diurnal variability of underwater acoustic noise characteristics in shallow water," *TELKOMNIKA Telecommunication, Computing, Electronics and Control*, vol. 15, no. 1, p. 314, 2017, doi: 10.12928/telkomnika.v15i1.4510.

- [25] L. M. Wolff, E. Szczepanski, and S. Badri-Hoher, "Acoustic underwater channel and network simulator," *IEEE Access*, vol. 8, pp. 136151-136175, 2020, doi: 10.1109/ACCESS.2020.3011620.
- [26] V. T. Vakily and M. Jannati, "A new method to improve performance of cooperative underwater acoustic wireless sensor networks via frequency controlled transmission based on length of data links," *Wireless Sensor Network*, vol. 2, no. 5, pp. 381-389, 2010, doi: 10.4236/wsn.2010.24050.
- [27] J. Iqbal, M. Jibrán, S. S. Ali, A. A. Rehmani, F. Ahmed, and S. A. Ali, "Differential sensitivity modeling & analysis of acoustic channel capacity in spectrum-aware underwater networks," *Proceedings of 2014 11th International Bhurban Conference on Applied Sciences & Technology (IBCAST) Islamabad, Pakistan, 14th - 18th January, 2014*, 2014, pp. 357-360, doi: 10.1109/IBCAST.2014.6778169.
- [28] M. Ghaleb, E. Felemban, A. A. Sheikh, and M. Felemban, "Design and performance analysis of underwater acoustic sensor networks," *Journal of Computational and Theoretical Nanoscience*, vol. 14, no. 1, pp. 347-353, 2017, doi: 10.1166/jctn.2017.6327.
- [29] M. Stojanovic, "On the relationship between capacity and distance in an underwater acoustic communication channel," *WUWNet '06: Proceedings of the 1st ACM international workshop on Underwater networks*, 2006, pp. 41-47, doi: 10.1145/1161039.1161049.
- [30] Al-Aboosi, Y. Yousif, H. Abdulrahem Taha, and H. Ali Abdualnabi. "Locally Optimal Detection of Signals in Underwater Acoustic Noise with Student's t-distribution," *IOP Conference Series: Materials Science and Engineering*, vol. 433, no. 1, p. 012086, 2018, doi: 10.1088/1757-899X/433/1/012086.
- [31] M. Lil and W. Zhao, "Review article on 1/f noise," *Mathematical Problems in Engineering*, vol. 2012, p. 673648, 2012, doi: 10.1155/2012/673648.
- [32] H. R. Gupta, R. Mehra, and S. Batan, "Power spectrum estimation using Welch method for various window techniques," *International Journal of Scientific Research Engineering and Technology (IJSRET)*, vol. 2, no. 6, pp. 389-392, 2013.
- [33] S. Kumar, P. Kumar, M. Gupta, and A. K. Nagawat, "Performance comparison of median and wiener filter in image de-noising," *International Journal of Computer Applications*, vol. 12, no. 4, pp. 27-31, 2010, doi: 10.5120/1664-2241.
- [34] J. S. G. Panaro, F. R. B. Lopes, L. M. Barreira, and F. E. Souza, "Underwater acoustic noise model for shallow water communications," *Brazilian telecommunication symposium*, 2012.
- [35] J. S. Panaro, F. R. Lopes, L. J. Matos, and L. M. Barreira, "Empirical noise model and likelihood metrics for underwater acoustic communications," *Proc. of the IEEE Conference on Underwater Communications Networking (UComms)*, 2012.
- [36] Y. Y. Al-Aboosi, A. Z. Sha'ameri, and A. H. Sallomi, "Enhancement signal detection in underwater acoustic noise using level dependent estimation time-frequency de-noising technique," *Journal of Marine Engineering & Technology*, vol. 19, no. 1, pp. 1-14, 2020, doi: 10.1080/20464177.2018.1508810.
- [37] R. P. Hodges, *Underwater acoustics: Analysis, design and performance of sonar*. John Wiley & Sons, 2011.

BIOGRAPHIES OF AUTHORS



Thamer Essa Murad    was born in Diyala-Iraq 1977. He received his B.Sc. degree in Electrical Engineering (General) in 2001-2002 from AL-Mustanseria University in Baghdad, Iraq. He is currently a master student's in electrical engineering department in AL-Mustanseria University. He can be contacted at email: thamer1977@gmail.com.



Yasin Yousif Al-Aboosi    received his BE degree in electronics and communication engineering from Baghdad University, Iraq, in 1995, and his ME degree in communication engineering from Technology University, Iraq, in 2003. He received his PhD degree from UTM, Malaysia, in 2017. He is currently an Assistant Professor at the Department of Electrical Engineering, College of Engineering, Mustansiriyah University, Iraq. His main research interests are underwater acoustic communication, signal processing, and medical image processing. He can be contacted at email: alaboosiyasin@gmail.com.